Available online at www.sciencedirect.com
ScienceDirect
International Journal of Mass Spectrometry 272 (2008) 154–164
International Journal of Mass Spectrometry
www.elsevier.com/locate/ijms

Electron ionization of CO_2

Simon J. King, Stephen D. Price *

Department of Chemistry, University College London, 20 Gordon Street, London WC1H 0AJ, UK

Received 9 December 2007; received in revised form 3 February 2008; accepted 4 February 2008
Available online 10 March 2008

Abstract

Relative partial ionization cross-sections (PICS) and precursor-specific relative partial ionization cross-sections for fragment ions formed by electron ionization of CO_2 have been measured using time-of-flight mass spectrometry (TOFMS) coupled with a 2-D ion-coincidence technique. We report data for the formation of C^+, O^+, CO^+, C^{2+}, O^{2+} and CO_2^{2+} relative to the formation of CO_2^+, as a function of ionizing electron energy from 30 to 200 eV. This data includes, for the first time, measurements on the formation of ion triples by dissociative multiple ionization of CO_2 by electrons. Our analysis of the 2-D coincidence spectra provides new information on the dynamics and energetic of charge separating dissociation of the CO_2 dication and trication. Through determinations of the kinetic energy release (KER) involved in ion pair formation, we also conclude that indirect double ionization processes contribute significantly to the yield of $CO^+ + O^+$ ion pairs at ionizing electron energies below 55 eV.

Keywords: Electron ionization; Partial ionization cross-sections; CO_2, Ion-coincidence; Multiple ionization

1. Introduction

Ionization of CO_2 is a process of importance in a number of planetary atmospheres [1–3] and plasma environments. Recent astrophysical models of the Martian atmosphere, where CO_2 is subject to magnetotail electron-ionization, predict an extensive ion-molecule chemistry involving the products of both dissociative and non-dissociative ionization [2]. Furthermore the existence of a CO_2^{2+} layer in the atmosphere of Mars has recently been predicted [3]. Such models require accurate and reliable data on the formation efficiency of both the parent ion and the various ionic fragments resulting from both single and multiple ionization. This information is often most conveniently expressed in the form of partial ionization cross-sections (PICS).

The dissociative ionization of CO_2 has been the subject of a number of investigations employing a variety of techniques: electron-ionization mass spectrometry [4–17], photoionization mass spectrometry [18–25], collisions with positrons [26], collisions with high translational energy ions [27], ultrafast laser pulses [28] and coincidence techniques [19–21,23–25,27,29,28]. Concentrating on the previous cross determinations for electron ionization of CO_2, the total ionization cross section has been measured from threshold to 100 eV by Asundi et al. [4] and from threshold to 1000 eV by Rapp and Englander-Golden [5]. The total dissociative ionization cross-section has been derived by Rapp et al. [6] via measurements of the number of ions formed with greater than 0.25 eV of translational kinetic energy. Cross-sections for the formation of CO_2^+ and CO_2^{2+} ions were reported by Märk and Hille [9] at an ionizing energy between threshold and 180 eV and absolute cross-sections for the formation of CO_2^+ ions were obtained by Freund et al. [11] for energies up to 200 eV. PICS for the formation of singly charged fragment ions CO^+, O^+ and C^+ have been measured, using a quadrupole mass spectrometer (QMS), by Crowe and McConkey [8] up to an ionizing energy of 300 eV and by Orient and Srivatava [10] in the energy range 10–510 eV. Straub et al. [14] measured PICS for the formation of singly and doubly charged ions from threshold to 1000 eV using a time-of-flight mass spectrometer (TOFMS) coupled with position sensitive ion detection. In this way Straub et al. [14] were able to demonstrate the complete collection of all ionic fragments, including those formed with considerable translational kinetic energy. Tian and Vidal [16] used a focusing time-of-flight mass spectrometer to measure PICS up to an electron energy of 300 eV and cross-sections for the formation of ion pairs up to 600 eV using a covariance mapping technique [15]. Comparison of these more recent determinations to the existing PICS data sets revealed some considerable discrepancies, particularly con-

* Corresponding author. Tel.: +44 20 7679 4606; fax: +44 20 7679 7463.
E-mail address: S.D.Price@ucl.ac.uk (S.D. Price).

1387-3806/$ – see front matter © 2008 Elsevier B.V. All rights reserved.
doi:10.1016/j.ijms.2008.02.008

cerning the formation of the fragment ions C^+ and O^+, for which the PICS values of Straub et al. [14] and Tian and Vidal [16] are considerably larger than those measured in previous studies. Such discrepancies were attributed to the inefficient collection of energetic ion fragments in these earlier determinations.

In this study, we investigate the electron ionization of CO_2 in the energy range 30–200 eV, using time-of-flight mass spectrometry coupled with a 2-D ion-coincidence technique. By this method single product ions, ion pairs and ion triples, formed following electron ionization of CO_2 are detected concomitantly, then identified and quantified. In this article, we report relative PICS $\sigma_r[X^{m+}]$ for the formation of C^+, O^+, CO^+, C^{2+}, O^{2+} and $CO_2{}^{2+}$ ions. This data is shown to be in excellent agreement with the existing PICS of Straub et al. [14] and Tian and Vidal [16]. We then present precursor-specific relative PICS $\sigma_n[X^{m+}]$, which, as shown by our recent studies of the electron ionization of C_2H_2 [30] and N_2O [31], quantify the contribution to the yield of a fragment ion from single ($n=1$), double ($n=2$) and triple ($n=3$) ionization. These precursor-specific relative PICS include, for the first time, measurements on the formation of ion triples following electron-ionization of CO_2.

Our 2-D ion-coincidence technique also provides information on the energetics and dissociation dynamics of the CO_2 dication and trication. The energies of the electronic states of $CO_2{}^{2+}$ have been extensively studied using photoion–photoion coincidence (PIPICO) spectroscopy [19–21,23,24], photoelectron–photoelectron coincidence (PEPECO) spectroscopy [32,29], threshold photoelectrons coincidence spectroscopy [33,29] (TPEsCO), double charge transfer (DCT) spectroscopy [34], position sensitive ion coincidence spectroscopy [17] and theoretical methods [21,35,36]. In this study, we report measurements of the kinetic energy release (KER) involved in ion pair formation following dissociative double ionization of CO_2. Using these measurements we also show that indirect processes play a significant role in ion pair formation close to the double ionization threshold.

2. Experimental

2.1. Experimental apparatus

All experiments in this study were performed using a TOFMS of Wiley-McLaren design, as has been discussed in detail in recent publications [37,31,30]. Electron ionization of a continuous effusive jet of CO_2 is performed by a pulsed beam of ionizing electrons with a duration 30 ns per pulse and a repetition rate of 50 kHz. We estimate that the energy resolution of the electron beam is 0.5 eV at full width at half maximum. Ion signals from a microchannel plate detector (MCP) are recorded as arrival times by a time-to-digital converter (TDC) capable of recording multiple stop signals per ionizing pulse. The arrival times of ions as single ion detections, or as ion pairs or ion triples, are accumulated in a memory module and transferred periodically to a PC. The CO_2 gas used in this work was a commercial sample of good purity (>99.8%).

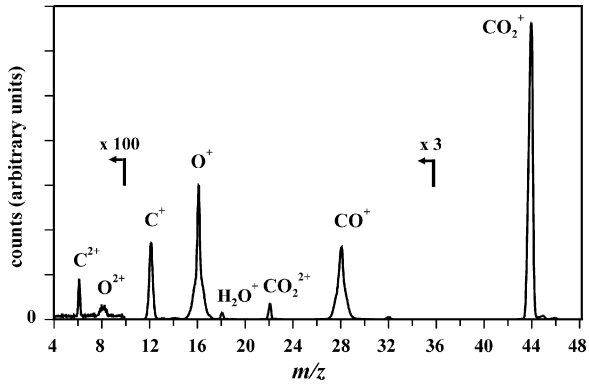

Fig. 1. A characteristic (singles) mass spectrum of CO_2 following electron impact ionization at 200 eV.

2.2. Experimental conditions

The operating conditions of our experiment involve low target gas pressures (<10^{-6} Torr) and low electron flux, ensuring that on average markedly less than one ionization event is detected per ionizing pulse of electrons. This methodology greatly reduces the number of 'false coincidences' that contribute to the coincidence spectra we record, as described below. False coincidences occur when two or more ions arising from separate ionization events are detected following a single ionizing pulse.

When extracting quantitative data from our experiment it is important that we detect all positively charged ions with equal efficiency, regardless of their mass, charge or initial kinetic energy. In a recent publication [30] we described a number of preliminary experiments performed using our apparatus, which demonstrate that we operate under conditions where mass discrimination effects do not influence our ion yields. Under the voltage conditions used in this study, ions will reach the detector provided they are formed with less than 11 eV of translational energy perpendicular to the TOF axis. Curtis and Eland [19] determined the total kinetic energy release from the dissociation of small molecular dications to be, commonly, less than 9 eV. Thus, in our experiment, conditions are optimised such that the majority of all ions formed by multiple ionization can be collected and indeed, as explained below, any small losses of energetic fragment ions from multiple ionization can be quantified and corrected.

2.3. Data processing

Single ion detections following a single ionizing pulse of electrons are termed 'singles' and are accumulated as a histogram of ion counts against time-of-flight to form a 'singles' mass spectrum (Fig. 1). The mass scale of the spectrum is calibrated by recording the mass spectrum of a reference species (Ar) under the same voltage conditions. The intensities of individual ion peaks, $I_1[X^+]$ for monocations and $I_2[X^{2+}]$ for dications in the mass spectrum, are then extracted by summing the counts in each peak after applying a small correction to account for the non-zero baseline due to background counts. Due

to the low target gas pressures employed in this study, as discussed above, a small number of ions emanating from traces of residual gases in our vacuum chamber contribute to our singles mass spectra. Specifically, ionization of residual O_2 and H_2O results in the formation of ions which contribute to the counts in our O^+ and O^{2+} peaks, while ionization of residual N_2 yields N_2^+ and N^+ ions which contribute to the counts in our CO^+ and CO^{2+} peaks, respectively. To quantify these background gas contributions we measured the yields of O^{2+}, O^+/O_2^{2+}, N^+ and N_2^+ ions with respect to O_2^+, and of O^{2+} and O^+ ions with respect to H_2O^+, by recording mass spectra of air and of H_2O under the same experimental conditions used in this study. A subtraction of the ions from the residual gases is made by normalization to the intensity of the O_2^+ peak and H_2O^+ peak in each CO_2 singles mass spectrum. This normalization procedure can only be performed by assuming that the formation of O_2^+ following ionization of CO_2 is negligible. To test this assumption we measured the yield of O_2^+ ions with respect to Ar^+ ions in all of our preliminary mass spectra of air. These ratios are in very good agreement to the ratio of O_2^+ to Ar^+ ions measured in all our CO_2 spectra, confirming that the formation of O_2^+ following ionization of CO_2 is negligible.

Events resulting in the detection of two ions and three ions following a single ionizing pulse of electrons, termed 'pairs' and 'triples', respectively, are stored and processed offline. In this work, we make a distinction between fragment ions comprising an ion pair formed via dissociative triple ionization $P_3[X^+]$, for example $C^+ + O^{2+}$, and ion pairs that may have contributions from both double and triple ionization $P_2[X^+]$, such as $C^+ + O^+$. Contributions from triple ionization to the intensities of such monocation pairs may arise when only two ions of an ion triple are detected, due to the less than unit detection efficiency of the apparatus. We neglect contributions to our coincidence spectra from dissociative quadruple ionization. Indeed, previous studies of the electron ionization of small molecules using this apparatus [31,30] indicate that such contributions are extremely small in the energy regime of this work.

Ion pairs are displayed as a 2-dimensional histogram of the respective ion flight times (t_1 vs. t_2), termed a 'pairs' spectrum (Fig. 2). The contribution of a fragment ion, for example $P_2[X^+]$, is obtained as the sum of the counts in all the appropriate peaks involving an X^+ ion. All of the peaks in our pairs spectra contain a small number of counts due to false coincidences, although this contribution is minimised experimentally by operating at low ion count rates as described above. False coincidence contributions to our pairs spectra are subtracted using an ion-autocorrelation function as has been described in the literature [30]. Typically false coincidences comprise 1–2% of the raw intensity of ion pair peaks at higher ionizing electron energy. A further correction is made to the intensity of the $O^+ + O^+$ and $O^{2+} + O^+$ peaks to account for the small contributions from ionization of residual O_2 in our vacuum chamber.

In our experiment no ion pairs are recorded if the second ion arrives at the detector within 32 ns of the first ion, due to the 'deadtime' of the discrimination circuitry. Such deadtime losses significantly affect the number of counts recorded in the $O^+ + O^+$ peak in our pairs spectra. To estimate the number of ions

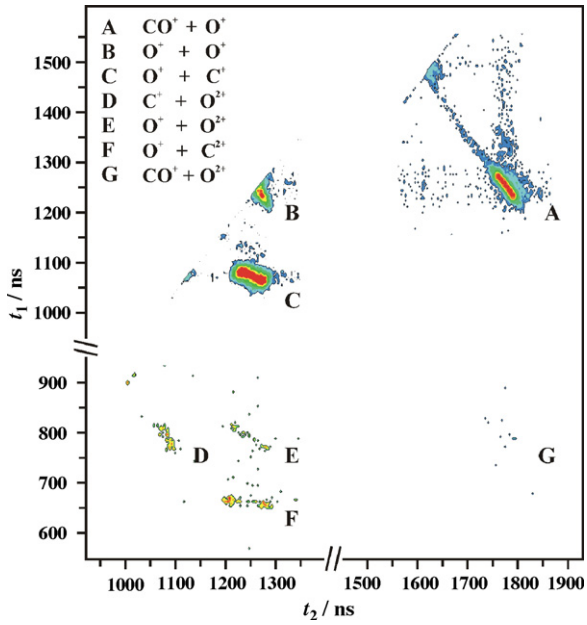

Fig. 2. Representative 'pairs' mass spectrum of CO_2 recorded at 200 eV showing observed ion pairs formed via dissociation of CO_2^{2+} and CO_2^{3+}.

lost, a separate 1-dimensional $(t_2 - t_1)$ spectrum is constructed from the $O^+ + O^+$ coincidence data and the coincidence data is appropriately extrapolated to the limit $t_1 = t_2$, using simple geometry, to correct for the losses.

In our pairs spectra we observe a 'tail' originating from the $CO^+ + O^+$ ion pair peaks, extending to the limit $t_1 = t_2 \approx 1545$ ns, arising from the slow dissociation of CO_2^{2+} ions in metastable states [15,38,29] (Fig. 2). These counts are included in the yields we measure for the formation of CO^+ and O^+ ions via dissociative double ionization. Metastable CO_2^{2+} ions which survive for at least 1500 ns will be recorded as single ion detections. Thus, the cross-sections we measure for the formation of CO_2^{2+} ions in this work are for CO_2^{2+} ions which have a lifetime longer than about 1500 ns.

Due to our neglect of quadruple ionization in this study, there is only one possible 'real' triple ion-coincidence, $C^+ + O^+ + O^+$. Ion triples are processed by specifying a time-of-flight range for a particular ion (C^+), and then extracting all ion triples containing at least one ion whose arrival time t_1 lies within this specified range. Once extracted, the respective flight times of the two remaining ions ($O^+ + O^+$) forming an ion triple are plotted as a 2-dimensional histogram (t_2 vs. t_3). The contribution of a fragment ion $T[X^+]$ is then obtained from the number of counts in the $O^+ + O^+$ peak, after applying a small geometric correction to account for losses due to the 'deadtime', as described above. False triple coincidences that contribute to the $C^+ + O^+ + O^+$ counts are subtracted using a procedure outlined in a recent publication [30].

As stated above, the voltage conditions employed in this study ensure the efficient collection of ions formed with up to 11 eV of translational energy aligned perpendicular to the TOF axis. In fact, the loss of energetic ions from multiple ionization appearing in our coincidence spectra, can easily be identified and corrected, if necessary, from the shape of the coincidence signals [37].

In this work, such corrections are used to quantify any losses of ion pairs formed via dissociative triple ionization. We note however that we are unable to correct for any losses of energetic monocations from single ionization, or dications from double ionization, if such fragment ions are formed with a kinetic energy greater than 11 eV. All ion intensities measured in this work were corrected numerically using the natural isotopic distributions.

2.4. Data reduction

The ion intensities measured in our spectra are processed to yield relative partial ionization cross-sections and precursor-specific relative PICS. Relative PICS, represented as $\sigma_r[X^+]$ for fragment monocations (X^+) and $\sigma_r[X^{2+}]$ for dications (X^{2+}), are all expressed relative to the cross-section for forming the parent monocation CO_2^+. Precursor-specific relative PICS are symbolized by $\sigma_n[X^+]$ and represent the relative cross-section for forming an ion (X^+) by single ($n=1$), double ($n=2$) or triple ($n=3$) ionization.

Our aim is to derive σ_r values for all the ions detected in our experiments. We recently reported an algorithm [30] showing that σ_r can be expressed in terms of the ion intensities recorded in our mass spectra. Relative PICS for the formation of fragment monocations (X^+) and dications (X^{2+}) using this algorithm are given by Eqs. (1)–(2).

$$\sigma_r[X^+] = \frac{I_1[X^+] + P_2[X^+] + P_3[X^+] + T[X^+]}{I[CO_2^+]} \quad (1)$$

$$\sigma_r[X^{2+}] = \frac{I_2[X^{2+}] + P_3[X^{2+}]}{I[CO_2^+]} \quad (2)$$

Precursor-specific relative PICS σ_n can be expressed in terms of the spectral intensities and the ion detection efficiency f_i. The ion detection efficiency must be considered to account for the transmission efficiency of the grids that define the electric fields in our apparatus, and also the efficiency of the detector and electronics. Precursor-specific relative PICS for the formation of fragment monocations (X^+), and dications (X^{2+}), are given below by Eqs. (3)–(5) and Eqs. (6)–(7), respectively. For the derivation of these equations the reader is referred to reference [30]. To measure the ion detection efficiency f_i separate experiments were performed, under the same voltage conditions employed in this study, to record the intensity of single ions and ion pairs formed by electron ionization of CF_4. Comparison of this data to the corresponding absolute measurements of Bruce and Bonham [39,40] yields a value of f_i, as has been described previously in the literature [37,31,30].

$$\sigma_1[X^+] = \frac{I[X^+] - ((1-f_i)/f_i)\left\{P_2[X^+] + P_3[X^+]\right\} + ((1-f_i)/f_i)^2 T[X^+]}{I[CO_2^+]} \quad (3)$$

$$\sigma_2[X^+] = \frac{(1/f_1)P_2[X^+] - 2((1-f_i)/f_i^2)T[X^+]}{I[CO_2^+]} \quad (4)$$

$$\sigma_3[X^+] = \frac{(1/f_i)P_3[X^+] + (1/f_i^2)T[X^+]}{I[CO_2^+]} \quad (5)$$

$$\sigma_2[X^{2+}] = \frac{I_2[X^{2+}] - ((1-f_i)/f_i)P_3[X^{2+}]}{I[CO_2^+]} \quad (6)$$

$$\sigma_3[X^{2+}] = \frac{(1/f_i)P_3[X^{2+}]}{I[CO_2^+]} \quad (7)$$

In our experiment only positive ions are detected and therefore the formation of positive ion–negative ion pairs, cannot be distinguished from the formation of a positive ion plus a neutral. However, estimates of the cross-section [41] for these processes are typically more than 3 orders of magnitude smaller than corresponding values of the total photoionization cross-section [23]. Therefore, we expect contributions from positive ion–negative ion pair formation to the cross-sections measured in this work to be minor.

2.5. Dication energetics: CO_2^{2+}

The shape of the peaks in the pairs spectrum can be interpreted to yield information on the kinetic energy released upon fragmentation of the carbon dioxide dication CO_2^{2+}. The kinetic energy release for a reaction is extracted by constructing a $(t_2 - t_1)$ plot from the experimental ion pair arrival times for an individual dissociation reaction and then performing a Monte-Carlo simulation of the dissociation process in the mass spectrometer. These Monte-Carlo simulations employ the full range of experimental variables, experimental conditions and reaction type which affect the simulated peak shape. The parameters of the simulated peak are then refined until a good fit to the experimental $(t_2 - t_1)$ plot is achieved.

Measurement of the KER enables the estimation of the precursor state energy $E(CO_2^{2+})$ of the carbon dioxide dication which dissociates to form the ion pair of interest, if the asymptotic energy E_{frag} of the dissociation limit is known or assumed:

$$E(CO_2^{2+}) = \mathrm{KER} + E_{frag} \quad (8)$$

Since the degree of internal excitation of the ionic fragments is often unknown, these estimates represent a lower limit for the electronic state energies of CO_2^{2+}. Despite this, such precursor state energies can provide valuable information on the energetics of dication dissociation processes.

3. Results

Mass and coincidence spectra of CO_2 were recorded at ionizing electron energies in the range 30–200 eV (Figs. 1 and 2). All spectra were processed, using the procedure described above, to yield σ_r values for the formation of the fragment monocations (C^+, O^+, CO^+) and dications (CO_2^{2+}, C^{2+}, O^{2+}) observed. These values are shown as a function of electron energy in Table 1 and Fig. 3 and represent the averages of three independent experimental determinations. Precursor-specific relative PICS σ_n for the formation of these ions were also derived, using the analysis

Table 1
Relative partial ionization cross-sections following electron ionization of CO_2, expressed relative to the cross-section for forming CO_2^+, as a function of electron energy E

E (eV)	$10^2\ \sigma_r[C^{2+}]$	$10^2\ \sigma_r[O^{2+}]$	$\sigma_r[C^+]$	$\sigma_r[O^+]$	$\sigma_r[CO_2^{2+}]$	$\sigma_r[CO^+]$
200	0.1387 (12)	0.0981 (37)	0.1517 (14)	0.3135 (22)	0.01448 (6)	0.1716 (14)
175	0.1218 (38)	0.0790 (65)	0.1528 (10)	0.3157 (17)	0.01444 (36)	0.1767 (24)
150	0.0941 (66)	0.0629 (72)	0.1533 (6)	0.3139 (15)	0.01452 (44)	0.1802 (21)
125	0.0629 (36)	0.0307 (54)	0.1498 (6)	0.3071 (8)	0.01399 (15)	0.1842 (15)
100	0.0289 (24)	0.0110 (32)	0.1415 (13)	0.2863 (7)	0.01275 (28)	0.1877 (13)
85	0.0117 (5)	0.0053 (16)	0.1326 (10)	0.2639 (23)	0.01102 (21)	0.1890 (14)
75	0.0043 (8)	0.0006 (12)	0.1239 (9)	0.2427 (9)	0.00934 (4)	0.1872 (19)
65	0.0004 (3)	0.0002 (2)	0.1110 (5)	0.2132 (13)	0.00678 (13)	0.1831 (6)
60	0.0000 (1)	−0.0002 (4)	0.1022 (1)	0.1947 (26)	0.00530 (3)	0.1806 (6)
55	−0.0000 (5)		0.0920 (9)	0.1775 (5)	0.00394 (3)	0.1733 (13)
50			0.0762 (1)	0.1498 (10)	0.00221 (5)	0.1645 (12)
45			0.0645 (5)	0.1324 (13)	0.00106 (2)	0.1614 (1)
40			0.0473 (15)	0.1161 (7)	0.00028 (3)	0.1633 (18)
35			0.0233 (10)	0.0985 (12)	0.00001 (1)	0.1576 (33)
30			0.0068 (3)	0.0788 (13)	−0.00000 (1)	0.1192 (44)

The value in parenthesis indicates the standard deviation in the last figure.

procedure outlined in Sections 2.3 and 2.4, and are displayed in Tables 2 and 3. The values of σ_1 and σ_2 are compared for all monocation fragments in Fig. 4 and the corresponding σ_3 values are shown in Fig. 5. The σ_2 and σ_3 values for dication fragments are shown in Fig. 6. We note here that while the magnitude of the absolute errors is comparable for all σ_n values reported in this study, the relative errors are considerably greater for our σ_3 values (Figs. 5 and 6) due to the low intensity of these disso-

Table 2
Relative *precursor-specific* PICS for forming monocation fragments following dissociative electron ionization of CO_2, expressed relative to the cross-section for forming CO_2^+, as a function of electron energy E

E (eV)	$\sigma_1[C^+]$	$\sigma_2[C^+]$	$\sigma_3[C^+]$	$\sigma_1[O^+]$	$\sigma_2[O^+]$	$\sigma_3[O^+]$
200	0.0979 (26)	0.0444 (14)	0.00944 (44)	0.1480 (54)	0.1461 (33)	0.0194 (11)
175	0.0994 (15)	0.0453 (2)	0.00814 (65)	0.1504 (30)	0.1487 (15)	0.0167 (15)
150	0.1017 (24)	0.0452 (12)	0.00651 (84)	0.1522 (27)	0.1484 (27)	0.0134 (17)
125	0.1039 (7)	0.0413 (5)	0.00459 (18)	0.1583 (26)	0.1394 (23)	0.0093 (3)
100	0.1063 (17)	0.0341 (5)	0.00108 (18)	0.1647 (26)	0.1194 (20)	0.0022 (4)
85	0.1080 (12)	0.0245 (4)	0.00020 (10)	0.1701 (29)	0.0935 (17)	0.0004 (2)
75	0.1079 (12)	0.0161 (4)	−0.00003 (3)	0.1734 (18)	0.0693 (10)	−0.0001 (1)
65	0.1037 (5)	0.0073 (2)		0.1710 (15)	0.0422 (3)	
60	0.0984 (0)	0.0038 (1)		0.1656 (28)	0.0291 (2)	
55	0.0904 (8)	0.0016 (1)		0.1590 (2)	0.0185 (3)	
50	0.0759 (1)	0.00029 (3)		0.1429 (13)	0.0070 (4)	
45	0.0645 (5)	0.00005 (1)		0.1305 (12)	0.0019 (3)	
40	0.0472 (15)	0.00007 (3)		0.1159 (5)	0.0002 (2)	
35	0.0232 (10)	0.00005 (3)		0.0985 (13)	0.0000 (1)	
30	0.0067 (3)	0.00007 (2)		0.0787 (15)	0.0001 (2)	

E (eV)	$\sigma_1[CO^+]$	$\sigma_2[CO^+]$	$\sigma_3[CO^+]$
200	0.0934 (24)	0.0781 (12)	0.00007 (1)
175	0.0966 (35)	0.0800 (13)	0.00003 (1)
150	0.1003 (30)	0.0799 (9)	0.00003 (2)
125	0.1068 (22)	0.0774 (8)	0.00002 (2)
100	0.1175 (16)	0.0703 (3)	0.00000 (1)
85	0.1283 (21)	0.0607 (9)	
75	0.1370 (23)	0.0502 (4)	
65	0.1485 (7)	0.0346 (2)	
60	0.1548 (8)	0.0258 (2)	
55	0.1555 (14)	0.0178 (2)	
50	0.1572 (13)	0.0072 (2)	
45	0.1589 (4)	0.0025 (2)	
40	0.1627 (19)	0.00065 (15)	
35	0.1574 (34)	0.00019 (10)	
30	0.1190 (45)	0.00023 (13)	

The value in parenthesis indicates the standard deviation in the last figure.

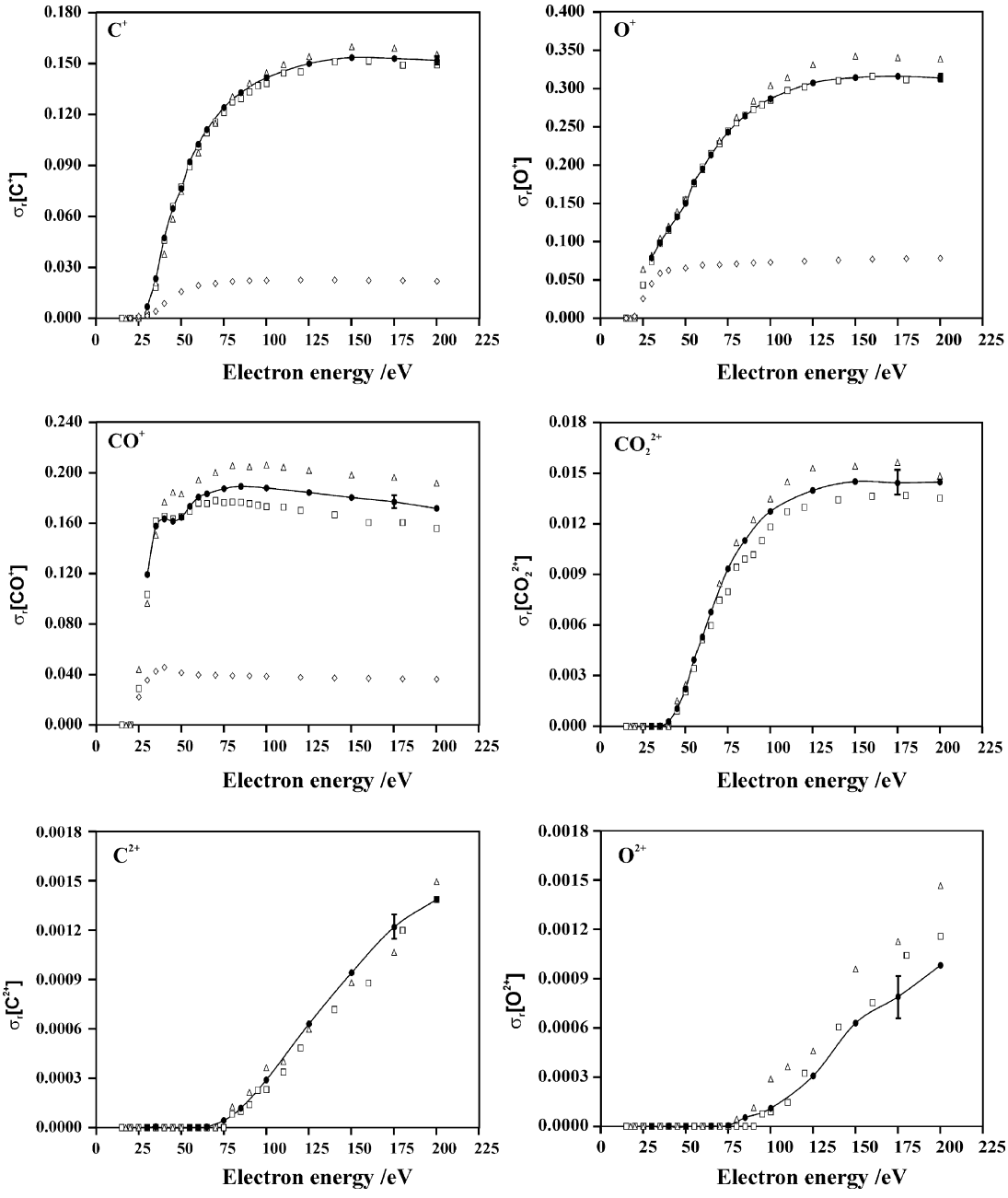

Fig. 3. Relative PICS $\sigma_r[X^{n+}]$ for forming fragment ions (●) following electron ionization of CO_2. The error bars expressed in this figure represent four standard deviations of three separate determinations. The corresponding relative PICS extracted from the data of Tian and Vidal [16] (△), Straub et al. [14] (□) and Zheng and Srivastava [10] (◊) are also shown.

ciative channels. The overall contributions from single, double and triple ionization, as a percentage of the total ion yield at each ionizing electron energy, are summarized in Table 4. From our data we estimate $\sigma_r[CO^{2+}]$ to be less than 0.0005 at all ionizing energies investigated in this study, in good agreement with the maximum limit suggested by Tian and Vidal [16]. Furthermore our singles mass spectra exhibit no discernible peaks attributable to the metastable CO_2^{3+} ion and we place an upper limit of 0.00002 on $\sigma_r[CO_2^{3+}]$.

As described above, to determine the ion detection efficiency (f_i) we recorded singles and pairs spectra of CF_4 at ionizing electron energies of 100 and 200 eV. Comparison of this data to the absolute cross-sections of Bruce and Bonham [39,40] resulted in a value of $f_i = 0.20 \pm 0.01$, in close agreement with previous determinations of f_i for our apparatus [19,31,30].

In our pairs spectra we observe 3 dissociation channels of CO_2^{2+}: $CO^+ + O^+$, $C^+ + O^+ + O$ and $O^+ + O^+ + C$. In addition, at electron energies above 75 eV we observe four ion pairs and one ion triple resulting from dissociation of CO_2^{3+}: $C^+ + O^{2+} + O$, $O^+ + O^{2+} + C$, $CO^+ + O^{2+}$, $O^+ + C^{2+} + O$ and $C^+ + O^+ + O^+$. The conclusions drawn from these coincidence signals concerning the energetics of dissociative double ionization of CO_2^{2+} (Section 4.3) and the dynamics of dissociative triple ionization of CO_2 (Section 4.4) are discussed below.

Table 3
Relative *precursor-specific* PICS for forming dication fragments following dissociative electron ionization of CO_2, expressed relative to the cross-section for forming CO_2^+, as a function of electron energy E

E (eV)	$10^3\ \sigma_2[C^{2+}]$	$10^3\ \sigma_3[C^{2+}]$	$10^3\ \sigma_2[O^{2+}]$	$10^3\ \sigma_3[O^{2+}]$
200	0.741 (120)	0.646 (124)	0.309 (35)	0.672 (69)
175	0.782 (76)	0.436 (48)	0.362 (75)	0.428 (80)
150	0.635 (104)	0.305 (48)	0.367 (111)	0.262 (52)
125	0.585 (40)	0.045 (15)	0.246 (64)	0.062 (25)
100	0.286 (27)	0.003 (4)	0.106 (26)	0.004 (6)
85	0.117 (4)	0.000 (2)	0.050 (10)	0.004 (6)
75	0.044 (8)		0.006 (9)	−0.001 (4)
65	0.003 (2)		0.003 (4)	
60	0.000 (3)		−0.002 (2)	
55				
50				
45				
40				
35				
30				

The value in parenthesis indicates the standard deviation in the last figure.

Table 4
Overall contributions from single, double and triple ionization, expressed as a percentage of the total ion yield, as a function of electron energy E

E (eV)	Single ionization	Double ionization	Triple ionization
200	81.0	17.2	1.8
175	81.0	17.4	1.5
150	81.4	17.4	1.2
125	82.7	16.5	0.8
100	85.2	14.5	0.2
85	88.1	11.9	0.0
75	90.7	9.3	0.0
65	94.0	6.0	0.0
60	95.7	4.3	0.0
55	97.1	2.9	0.0
50	98.8	1.2	0.0
45	99.6	0.4	0.0
40	99.9	0.1	0.0
35	100.0	0.0	0.0
30	100.0	0.0	0.0

4. Discussion

4.1. Relative partial ionization cross-sections

The values of $\sigma_r[X^+]$ we determine for the formation of monocation fragments ($X^+ = CO^+, O^+, C^+$), are shown in Fig. 3. Over the entire ionizing energy range there is excellent agreement between our $\sigma_r[X^+]$ values and the values derived from the data of Straub et al. [14] and Tian and Vidal [16]. Both of these previous studies efficiently collected ion fragments with considerable translational kinetic energy, and hence, the close agreement between these data sets and our $\sigma_r[X^+]$ values demonstrate the expected efficient collection of such energetic ion fragments in our apparatus. By contrast, the $\sigma_r[X^+]$ values for the formation of these monocation fragments derived from the data of Orient and Srivastava [10] lie considerably lower than these data sets. The lower PICS measurements for the formation of CO^+, O^+ and C^+ by Orient and Srivastava [10], and in previous studies [8], can be explained [16] by the inefficient collection of ionic fragments formed with a translational energy in excess of a few electron Volts.

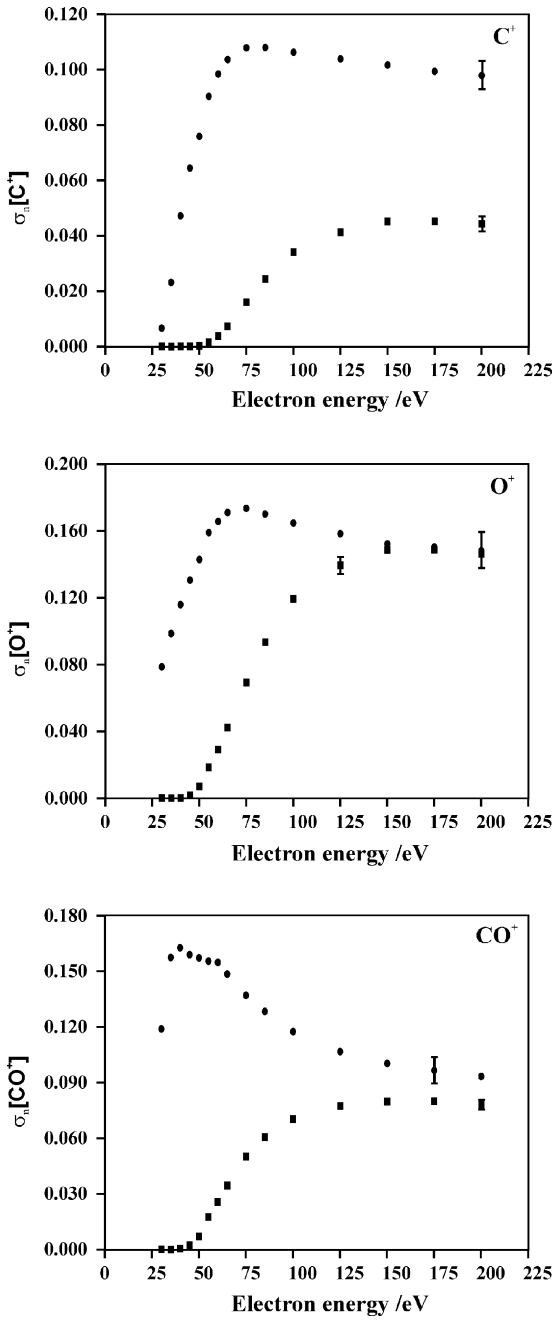

Fig. 4. Relative precursor-specific PICS for forming monocation fragments via single ionization (●), and via double ionization (■), following electron ionization of CO_2. The representative error bars show four standard deviations of three separate determinations.

Comparing Fig. 3 the values of $\sigma_r[C^{2+}]$ we determine for the formation of dication fragments to the corresponding values derived from the data of Straub et al. [14] and Tian and Vidal [16] shows excellent agreement. A similar comparison of $\sigma_r[O^{2+}]$ values reveals a good agreement between our measurements and the data of Straub et al. [14] Our $\sigma_r[O^{2+}]$ values are on average around 30% smaller than the values derived from the data of

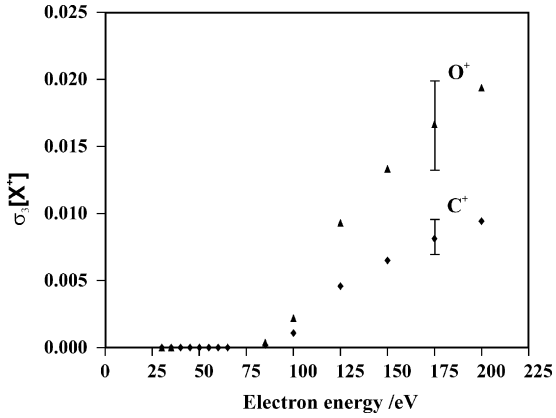

Fig. 5. Relative precursor-specific PICS for forming monocation fragments C^+ (♦) and O^+ (▲) via triple ionization, following electron ionization of CO_2. The representative error bars show four standard deviations of three separate determinations.

Tian and Vidal [16], but both data sets agree within their mutual error limits.

4.2. Relative precursor-specific PICS

Unless noted below, our values for σ_1 and σ_2 for the different fragment ions are in good agreement with values extracted from the existing covariance mapping data of Tian and Vidal [15]. We note that no values of σ_3 for the different fragment ions involving the detection of ion triples have been determined before.

Comparison of our $\sigma_1[CO^+]$ and $\sigma_2[CO^+]$ values Fig. 4 to the data of Tian and Vidal [15] reveals that at ionizing energies above 100 eV, the contribution of CO^+ ions from double ionization is significantly larger than reported previously, whereas contributions to the CO^+ ion yield from single ionization are lower. The origin of this discrepancy is not readily apparent. One possible explanation for these differences is that Tian and Vidal extracted the various fragment ion yields from dissociative single and double ionization using data recorded in two separate studies, whereas in this study ion 'singles' mass spectra and coincidence spectra were recorded concomitantly and are thus by definition mutually consistent.

A comparison of our $\sigma_1[O^+]$ values, above 75 eV, to the data of Tian and Vidal [15] again reveals a less satisfactory agreement than is generally the case for σ_1 and σ_2 for other fragment ions. Again, these differences may arise from the acquisition of separate conventional mass spectra and ion-coincidence spectra by Tian and Vidal.

In Fig. 6 we see that contributions to the C^{2+} ion yield are from both double and triple ionization. From our $\sigma_2[C^{2+}]$ values we determine a threshold for C^{2+} formation at 72 ± 3 eV, in good agreement with previous determinations [12,16]. Recently, Straub et al. [14] showed that at 200 eV C^{2+} ions are formed with a near-thermal kinetic energy distribution. On this basis it was proposed that the most likely mechanism for forming C^{2+} ions at this ionizing energy was via dissociative double ionization. However, our measurements show that at 200 eV contributions to the C^{2+} ion yield are from both double and triple ionization in almost equal proportions. Thus, C^{2+} ions are formed with very low translational kinetic energy from both double and triple ionization.

In Fig. 6 we show that contributions to the O^{2+} ion yield are from both double and triple ionization. From our $\sigma_2[O^{2+}]$ values we determine a threshold for O^{2+} formation at 74 ± 3 eV, again in good agreement with a previous determination [16]. At 200 eV contributions to the O^{2+} ion yield from triple ionization are far greater than from double ionization. Comparison of this data to values derived from the data of Tian and Vidal [15] shows that both our $\sigma_2[O^{2+}]$ values and $\sigma_3[O^{2+}]$ values are slightly lower than reported previously.

4.3. The energetics of dissociative double ionization

The kinetic energy of the ion pairs formed by dissociation of the $CO_2{}^{2+}$ dication have been determined using Monte-Carlo simulations of the peaks we observe in the pairs spectrum, as described in Section 2.5. All KER determinations were made from data recorded at electron energies above 50 eV, as the coincidence spectra recorded at electron energies lower than 50 eV contained insufficient coincidence signals to produce statistically significant results. In these simulations all KER components were modelled using a Gaussian distribution with a

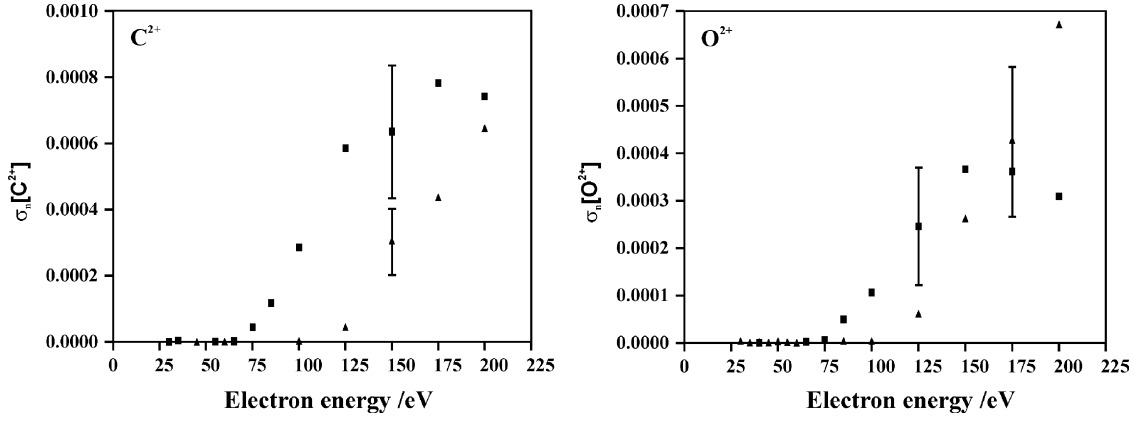

Fig. 6. Relative precursor-specific PICS for forming dication fragments via double ionization (■), and via triple ionization (▲), following electron ionization of CO_2. The representative error bars show four standard deviations of three separate determinations.

width of 1.2 eV at FWHM [24]. In the sections that follow here we compare our KER measurements with available experimental and theoretical data.

4.3.1. $CO^+ + O^+$

The formation of $CO^+ + O^+$ ion pairs is the dominant dication dissociation channel at all ionizing energies investigated in this study above the double ionization threshold. For $CO^+ + O^+$, the slope of peaks appearing in our pairs spectra, reassuringly, all lie close to −1, as required for a simple two-body dissociation process [42]. For this ion pair at 50 eV we determine a single-valued kinetic energy release of 4.4 ± 0.4 eV and this KER component increases to 5.0 ± 0.5 eV at 65 eV. Furthermore, at ionizing energies in excess of 50 eV, a second discrete KER of 7.5 ± 0.5 eV is observed. The weighting of this second KER increases from 15% to 35% between 55 and 75 eV. Our values of the KER in the ionizing energy range 50–75 eV are in good agreement with corresponding data from earlier PIPICO measurements of Dujardin and Winkoun [20], who determined a single-valued KER of 4.5 eV at a photon energy of 40.5 eV, and noted the emergence of a second KER component of 6.5 eV at photon energies above 43.5 eV. Curtis and Eland [19] determined a single-valued kinetic energy release of 6.0 ± 0.3 eV, with a very broad distribution (3 eV FWHM), using the PIPICO technique at a photon ionizing energy of 40.8 eV. If we compare our values for the average KER, 5.8 ± 0.4 eV at 65 eV and 5.9 ± 0.4 eV at 75 eV, with the values of Curtis and Eland [19], good agreement is found. Our KER measurements do not agree quite as well with a more recent PIPICO investigation by Masuoka et al. [24], who used a curve fitting procedure to extract the kinetic energy release distribution of $CO^+ + O^+$ ion pairs formed by photoionization in the energy range 40–100 eV.

Our kinetic energy release obtained at 50 eV, assuming the formation of ground state products CO^+ ($^2\Sigma^+$) + O^+ (^4S_u), a dissociation limit which lies at 33.15 eV [43,44] with respect to CO_2 in its ground state ($X^1\Sigma_g^+$), suggests a dissociative precursor state lying at 37.55 ± 0.4 eV. Previous measurements of the appearance potential for $CO^+ + O^+$ formation have been reported by Masuoka [23] (39.2 ± 0.3 eV) and by Millie et al. [21] (39.7 ± 0.5 eV), using the PIPICO method, and by Slattery et al. [29] (38.65–38.80 eV) using TPEsCO spectroscopy coupled with an ion-coincidence technique. Of these previous experimental studies, only the TPEsCO-ion–ion-coincidence technique of Slattery et al. [29] selectively probes $CO^+ + O^+$ ion pairs formed exclusively via direct dissociative double ionization. Theory similarly predicts a barrier to $CO^+ + O^+$ formation on the ground $^3\Sigma_g^-$ surface of the CO_2^{2+} dication at 38.7 eV [36]. The lower precursor state energy we observe suggests that we are sampling indirect processes contributing significantly to the $CO^+ + O^+$ ion yield from states lying below the threshold for direct ion pair formation. Indeed, recent TOF-PEPECO measurements [29] have observed $CO^+ + O^+$ formation below the double ionization threshold, involving autoionization of oxygen atoms:

$$CO_2 + e^- \rightarrow CO_2^{*+} + 2e^- \rightarrow CO^+ + O^* + 2e^- \rightarrow CO^+ + O^+ + 3e^- \quad (1)$$

Using this PEPECO data, Slattery et al. [29] proposed a threshold for indirect formation of $CO^+ + O^+$ ion pairs of 35.56 ± 0.10 eV, below even the threshold we determine for 50 eV electrons. The second KER component we observe at ionizing energies above 55 eV, measured as 7.5 ± 0.5 eV, implies a precursor state energy lying higher in the electronic state manifold of CO_2^{2+} at 40.65 ± 0.5 eV.

4.3.2. $C^+ + O^+ + O$

Tian and Vidal [15] described the formation of $C^+ + O^+ + O$ ion pairs from CO_2^{2+} as a secondary decay process, as shown in Eq. (2):

$$CO_2^{2+} \rightarrow CO^+ + O^+ \rightarrow O + C^+ + O^+ \quad (2)$$

The peak slopes we measure for this ion pair lie close to −0.43 below 65 eV, then increase gradually with increasing electron energy (−0.34 at 100 eV, −0.26 at 200 eV). In addition, we observe a broadening of the $C^+ + O^+$ ion pair peak in our pairs spectra, with increasing ionizing energy. Tian and Vidal [15] attributed this broadening of the ion pair signals to an increasing contribution from concerted processes involving higher electronic states of CO_2^{2+}. For secondary decay of CO^+ to $C^+ + O$, with no kinetic energy release in the secondary step, the peak slope is expected [42] to be −0.43, as we observe within experimental error below 65 eV. For a concerted process forming $C^+ + O^+$ ion pairs, the peak slope should lie between −0.43 and −1, depending on whether the dissociation process involves a head-on-collision or an unobstructed instantaneous Coulomb explosion [42]. Thus, if concerted processes contribute significantly to the $C^+ + O^+$ ion yield with increasing ionization energy, as proposed by Tian and Vidal [15], we would expect values of the peak slope to decrease from −0.43 towards −1. The gradual increase in peak slope values that we observe above 65 eV can be explained by the growth of a small component of aligned energy release [42] in the secondary decay step. This aligned secondary KER, coupled with small deviations from linearity in this three-body dissociation process, may also give rise to the observed broadening of $C^+ + O^+$ ion pair peaks in the pairs spectra.

From a Monte-Carlo simulation of the coincidence data for this ion pair at 60 eV we determine two components of kinetic energy release, 6.0 ± 0.5 and 9.5 ± 0.5 eV, with weightings of 7:3. The asymptote for the formation of ground state products C^+ (^2P_u) + O^+ (^4S_u) + O (^3P_g) lies at 41.55 eV [43,44], suggesting precursor states for $C^+ + O^+$ formation at 47.55 ± 0.5 and 51.05 ± 0.5 eV, respectively. The lower of these values is in good agreement with previous measurements of the appearance potential for forming $C^+ + O^+$ via photoionization [21,23].

4.3.3. $O^+ + O^+ + C$

In our experimental setup, due to the deadtime of the discrimination circuitry, kinetic energy release determinations cannot be easily performed for monocation pairs with identical mass. Despite this, by manually fitting a straight line to the visible portion of $O^+ + O^+$ ion pair peaks, observed in our pairs spectra at higher ionizing energies (Fig. 2), we determine peak slopes

all lying close to −1. These measurements are consistent with a concerted mechanism for forming $O^+ + O^+$ ion pairs.

4.4. Dissociation of CO_2^{3+}

In our coincidence mass spectra recorded at 200 eV we observe four ion pairs and one ion triple arising from the dissociation of the carbon dioxide trication CO_2^{3+}. Our data shows that dissociation of CO_2^{3+} to form an ion triple, $C^+ + O^+ + O^+$, is the most abundant trication dissociation channel at all ionizing energies investigated in this study. Indeed, the propensity of symmetric charge separation among the ion fragments formed upon dissociative multiple ionization of CO_2 has been observed previously, in studies using intense laser pulses [28] and involving collisions with high energy ions [27,45].

The peak slopes we measure for $O^{2+} + O^+$ ion pairs above 125 eV all lie close to −0.50. Assuming that this dissociation reaction is approximately linear, our peak slopes suggest the formation of $O^{2+} + O^+ + C$ is via a concerted process [46], in which the central C atom remains almost stationary. For the formation of $O^{2+} + CO^+$ ion pairs our peak slopes similarly all lie close to −0.50, as predicted for a two-body dissociation process. For $C^{2+} + O^+$ formation we determine a peak slope close to −0.10 at ionizing energies above 125 eV. If this reaction were to proceed via an instantaneous Coulomb explosion, where the central C^{2+} ion is obstructed by the neutral O atom, we would predict a minimum peak slope of −0.21. The peak slopes that we measure show that the C^{2+} ion carries a much smaller component of momentum than predicted for an instantaneous explosion reaction [15]. For dissociation of CO_2^{3+} into $O^{2+} + C^+$ ion pairs, we measure peak slope values of around −1.40. If this reaction were to proceed via an instantaneous explosion, in which the departing C^+ ion is obstructed by the neutral O atom, we predict a maximum peak slope of −1.17. This again suggests that the momentum partitioned to the central carbon ion is much lower than is predicted for a concerted process. This feature of the fragmentation of CO_2^{3+} has been explained previously [15] by using the charge exchange model of Hsieh and Eland [47].

5. Conclusions

Time-of flight mass spectrometry coupled with a 2-D ion-coincidence technique has been used to measure relative partial ionization cross-sections for the formation of positively charged ions following electron ionization of CO_2 in the energy range 30–200 eV. Using this methodology we have also derived relative precursor-specific PICS, which enable us to quantify the contribution to the yield of each fragment ion from single, double and triple ionization. These measurements include, for the first time, contributions from ion triples formed by dissociative electron ionization.

Excellent agreement is found between our data and two recent determinations of the PICS of CO_2. Our relative precursor-specific PICS reveal that contributions to the C^+ ion yield are dominated by dissociative single ionization across the ionizing energy range. By contrast, contributions to the yield of O^+ and CO^+ fragments ions from dissociative double ionization, are comparable to contributions from dissociative single ionization above 100 eV. We also show that contributions to the yield of fragment dications, C^{2+} and O^{2+}, are from both double and triple ionization. Fragment ions formed via dissociative triple ionization are shown to comprise 1.8% of the total ion yield at 200 eV, much greater than reported previously.

The analysis of the 2-D coincidence spectra provides information on the dynamics and energetics of charge separating dissociation of the CO_2^{2+} dication. We conclude that indirect double ionization contributes significantly to the yield of $CO^+ + O^+$ pairs at electron energies below 55 eV. In our analysis of the dissociation of CO_2^{3+}, we observe a propensity of symmetric charge separation among the ion fragments leading to the formation ion triples.

Acknowledgements

The authors acknowledge helpful discussions with Tilmann Märk and Paul Scheier regarding the collection of energetic ions in experiments determining partial ionization cross-sections. In addition the authors would like to acknowledge an EPSRC studentship for SJK.

References

[1] S.A. Haider, Indian J. Radio Space Phys. 17 (1988) 183.
[2] S.A. Haider, J. Geophys. Res.-Space Phys. 102 (1997) 407.
[3] O. Witasse, O. Dutuit, J. Lilensten, R. Thissen, J. Zabka, C. Alcaraz, P.L. Blelly, S.W. Bougher, S. Engel, L.H. Andersen, K. Seiersen, Geophys. Res. Lett. 29 (2002).
[4] R.K. Asundi, M.V. Kurepa, J.D. Craggs, Proc. Phys. Soc. Lond. 82 (1963) 967.
[5] D. Rapp, P.J. Englande, Chem. Phys. 43 (1965) 1464.
[6] D. Rapp, P. Englande, D.D. Briglia, J. Chem. Phys. 42 (1965) 4081.
[7] R.G. Cooks, Dt. Terwilli, J.H. Beynon, J. Chem. Phys. 61 (1974) 1208.
[8] A. Crowe, J.W. McConkey, J. Phys. B-At. Mol. Opt. Phys. 7 (1974) 349.
[9] T.D. Mark, E. Hille, J. Chem. Phys. 69 (1978) 2492.
[10] O.J. Orient, S.K. Srivastava, J. Phys. B-At. Mol. Opt. Phys. 20 (1987) 3923.
[11] R.S. Freund, R.C. Wetzel, R.J. Shul, Phys. Rev. A 41 (1990) 5861.
[12] R. Velotta, P. Digirolamo, V. Berardi, N. Spinelli, M. Armenante, J. Phys. B-At. Mol. Opt. Phys. 27 (1994) 2051.
[13] R. Locht, M. Davister, Int. J. Mass Spectrom. Ion Process. 144 (1995) 105.
[14] H.C. Straub, B.G. Lindsay, K.A. Smith, R.F. Stebbings, J. Chem. Phys. 105 (1996) 4015.
[15] C.C. Tian, C.R. Vidal, Phys. Rev. A 58 (1998) 3783.
[16] C.C. Tian, C.R. Vidal, J. Chem. Phys. 108 (1998) 927.
[17] B. Bapat, V. Sharma, J. Phys. B-At. Mol. Opt. Phys. 40 (2007) 13.
[18] B.P. Tsai, J.H.D. Eland, Int. J. Mass Spectrom. Ion Process. 36 (1980) 143.
[19] D.M. Curtis, J.H.D. Eland, Int. J. Mass Spectrom. Ion Process. 63 (1985) 241.
[20] G. Dujardin, D. Winkoun, J. Chem. Phys. 83 (1985) 6222.
[21] P. Millie, I. Nenner, P. Archirel, P. Lablanquie, P. Fournier, J.H.D. Eland, J. Chem. Phys. 84 (1986) 1259.
[22] R. Locht, M. Davister, W. Denzer, H.W. Jochims, H. Baumgartel, Chem. Phys. 138 (1989) 433.
[23] T. Masuoka, Phys. Rev. A 50 (1994) 3886.
[24] T. Masuoka, E. Nakamura, A. Hiraya, J. Chem. Phys. 104 (1996) 6200.
[25] T. Masuoka, J. Electron. Spectrosc. Relat. Phenom. 103 (1999) 53.
[26] H. Bluhme, N.P. Frandsen, F.M. Jacobsen, H. Knudsen, J.P. Merrison, R. Mitchell, K. Paludan, M.R. Poulsen, J. Phys. B-At. Mol. Opt. Phys. 32 (1999) 5825.
[27] J.H. Sanderson, T. Nishide, H. Shiromaru, Y. Achiba, N. Kobayashi, Phys. Rev. A 59 (1999) 4817.

[28] J.P. Brichta, S.J. Walker, R. Helsten, J.H. Sanderson, J. Phys. B-At. Mol. Opt. Phys. 40 (2007) 117.
[29] A.E. Slattery, T.A. Field, M. Ahmad, R.I. Hall, J. Lambourne, F. Penent, P. Lablanquie, J.H.D. Eland, J. Chem. Phys. 122 (2005).
[30] S.J. King, S.D. Price, J. Chem. Phys. 127 (2007) 174307.
[31] N.A. Love, S.D. Price, Phys. Chem. Chem. Phys. 6 (2004) 4558.
[32] J.H.D. Eland, Chem. Phys. 294 (2003) 171.
[33] R.I. Hall, L. Avaldi, G. Dawber, A.G. McConkey, M.A. Macdonald, G.C. King, Chem. Phys. 187 (1994) 125.
[34] M.L. Langford, F.M. Harris, C.J. Reid, J.A. Ballantine, D.E. Parry, Chem. Phys. 149 (1991) 445.
[35] H. Hogreve, J. Phys. B-At. Mol. Opt. Phys. 28 (1995) L263.
[36] M. Hochlaf, F.R. Bennett, G. Chambaud, P. Rosmus, J. Phys. B-At. Mol. Opt. Phys. 31 (1998) 2163.
[37] S. Harper, P. Calandra, S.D. Price, Phys. Chem. Chem. Phys. 3 (2001) 741.
[38] D. Schroder, H. Schwarz, J. Phys. Chem. A 103 (1999) 7385.
[39] M.R. Bruce, R.A. Bonham, Int. J. Mass Spectrom. Ion Process. 123 (1993) 97.
[40] M.R. Bruce, L. Mi, C.R. Sporleder, R.A. Bonham, J. Phys. B-At. Mol. Opt. Phys. 27 (1994) 5773.
[41] K. Mitsuke, S. Suzuki, T. Imamura, I. Koyano, J. Chem. Phys. 93 (1990) 1710.
[42] J.H.D. Eland, Mol. Phys. 61 (1987) 725.
[43] H.Y. Afeefy, J.F. Liebman, and S.E. Stein, "Neutral Thermochemical Data" in NIST Chemistry WebBook, NIST Standard Reference Database Number 69, Eds. P.J. Linstrom and W.G. Mallard, June 2005, National Institute of Standards and Technology, Gaithersburg MD, 20899 (http://webbook.nist.gov).
[44] S.G. Lias, J.E. Bartmess, J.F. Liebman, J.L. Holmes, R.D. Levin, and W.G. Mallard in "Ion Energetics Data" NIST Chemistry WebBook, NIST Standard Reference Database Number 69, Eds. P.J. Linstrom and W.G. Mallard, June 2005, National Institute of Standards and Technology, Gaithersburg MD, 20899 (http://webbook.nist.gov).
[45] D. Mathur, Phys. Rep.-Rev. Sect. Phys. Lett. 391 (2004) 1.
[46] J.H.D. Eland, in: C.Y. Ng (Ed.), Vacuum Ultraviolet Photonionization and Photodissociation of Molecules and Clusters, World Scientific, Singapore, 1991.
[47] S. Hsieh, J.H.D. Eland, J. Chem. Phys. 103 (1995) 1006.